

Assessment of property profile of post-industrial polypropylene recyclates through a multivariable recycling process

Mohamad Hassan Akhras^{1,2}  | Christian Marschik¹  | Chi Nghia Chung¹ | Ines Traxler¹  | Konstanze Kruta¹ | Karin Kloiber¹ | Joerg Fischer² 

¹Competence Center CHASE GmbH, Linz, Austria

²Johannes Kepler University Linz, Institute of Polymeric Materials and Testing, Linz, Austria

Correspondence

Christian Marschik, Competence Center CHASE GmbH, Hafenstrasse 47-51, 4020 Linz, Austria.
Email: christian.marschik@chasecenter.at

Funding information

COMET-Competence Centers for Excellent Technologies programme, Grant/Award Number: 868615; Johannes Kepler Open Access Publishing Fund, Grant/Award Number: 868615

Abstract

This study provides key insights into the extrusion of a post-industrial feedstock primarily composed of polypropylene (PP) and reveals its influence on the property profile of the recyclate. The objective of this study was to gain a fundamental understanding of complex process-property relationships. Therefore, a two-part experimental design was established. The first part aimed to analyze the feedstock variability by investigating key material properties of recyclates produced under constant processing conditions. The second part aimed to systematically evaluate the effect of the screw speed, filtration setup, and degassing setup on the properties of the recyclates. An industrial-scale recycling extrusion line was used. The material evaluation included melt mass-flow rate (MFR), ash content, oxidation induction temperature, tensile and impact properties, degassing performance, and residual volatile organic compounds (VOCs). Higher melt temperatures led to chain scission of the PP fraction, resulting in increased MFR and higher material stiffness. Additionally, a finer filtration positively contributed to the enhanced material stiffness. Furthermore, the mechanical properties were also influenced by the levels of inorganic fillers in the material composition of the feedstock. Finally, the filtration setup had a greater impact on degassing performance and residual VOC levels than the degassing setup and screw speed.

KEYWORDS

extrusion, polyolefins, recycling

1 | INTRODUCTION

Plastics recycling has gained a significant momentum in recent years, emerging as one of the most viable recovery methods for plastic waste.¹ In 2008, the European

Parliament introduced 37 Directive 2008/98/EC to the member states that aims at maximizing the reuse and recycling of 38 plastic waste.² These recycling targets were subsequently reinforced in 2018 by Directive 392,018/851, with the goal of achieving recycling rates of

This is an open access article under the terms of the [Creative Commons Attribution](https://creativecommons.org/licenses/by/4.0/) License, which permits use, distribution and reproduction in any medium, provided the original work is properly cited.

© 2024 The Author(s). *Journal of Applied Polymer Science* published by Wiley Periodicals LLC.

55% by the end of 2025 and 60% by the end of 2030.³ This imposed substantial pressure on the plastics industry, driving the development of innovative solutions to improve recycling processes, and consequently, elevate the recycling rates and enhance the quality of recycled plastics. Plastic waste is fundamentally categorized based on its source, distinguishing between post-industrial and post-consumer waste.⁴ Post-industrial waste originates from production residues and never reaches the end consumer (e.g., injection molding sprues), thus it is typically less contaminated making it readily recyclable,^{1,5-7} while post-consumer waste is generated after the use-phase and disposal.⁵ The term “recovery” in the context of plastic wastes encompasses all methods of reclaiming plastic waste, including recycling, regardless of the waste type.^{4,8} Among the various approaches, mechanical recycling is widely regarded as one of the most efficient and effective practices.⁹⁻¹¹ Mechanical recycling typically involves techniques that transform plastic waste into secondary raw materials using physical processes such as shredding and extrusion.^{1,10}

The mechanical recycling process typically commences with the collection of the plastic waste and ends with the regranulation step.^{1,10} Nevertheless, prior to entering regranulation, several supplementary steps, such as sorting, shredding, washing, and drying, are frequently conducted to enhance the homogeneity of the input materials and, consequently, the quality of the resulting recyclates.^{6,8} Therefore, mechanical recycling can be conceptually categorized into two stages: (i) the preparatory stage, which yields pretreated flakes, and (ii) the regranulation stage, responsible for transforming these flakes into recyclates. The regranulation of plastic waste into pellets through extrusion stands out as the most commonly employed recycling technology. This popularity is attributed to its cost-effectiveness, versatility with various polymer types, high efficiency, and the potential to enhance polymer melt quality by incorporating filtration and degassing units into the extrusion process.¹¹⁻¹³

The extrusion process plays a crucial role in the mechanical recycling of plastics and has a significant influence on the properties of the resulting recyclates. Its influence stems from the capacity of the extrusion process to enhance the quality and homogeneity of the polymer via processing steps such as melting, filtering the polymer melt, degassing, and mixing.¹³⁻¹⁵ For instance, employing an appropriate filtration system can effectively eliminate larger non-volatile contaminants such as dust, gel particles, and foreign polymers. This in turn improves the homogeneity of the polymer and, consequently, enhances the mechanical and optical properties of the recyclates.^{11,15} Furthermore, the use of a degassing unit facilitates the removal of volatile compounds, effectively

reducing processes like hydrolysis and acidolysis, thus ultimately improving the odor of the resulting recyclate and increasing its value.^{11,13,14} Nevertheless, it must be noted that mechanical recycling also entails harmful effects on the polymers.¹⁶ Plastic waste materials, especially thermoplastics, are inevitably subjected to degradation (e.g., thermal and mechanical) due to exposure to process-induced stresses when they are reintroduced into production processes, which in turn triggers irreversible alterations in the material structure and properties, limiting their suitability for certain applications.^{10,16,17}

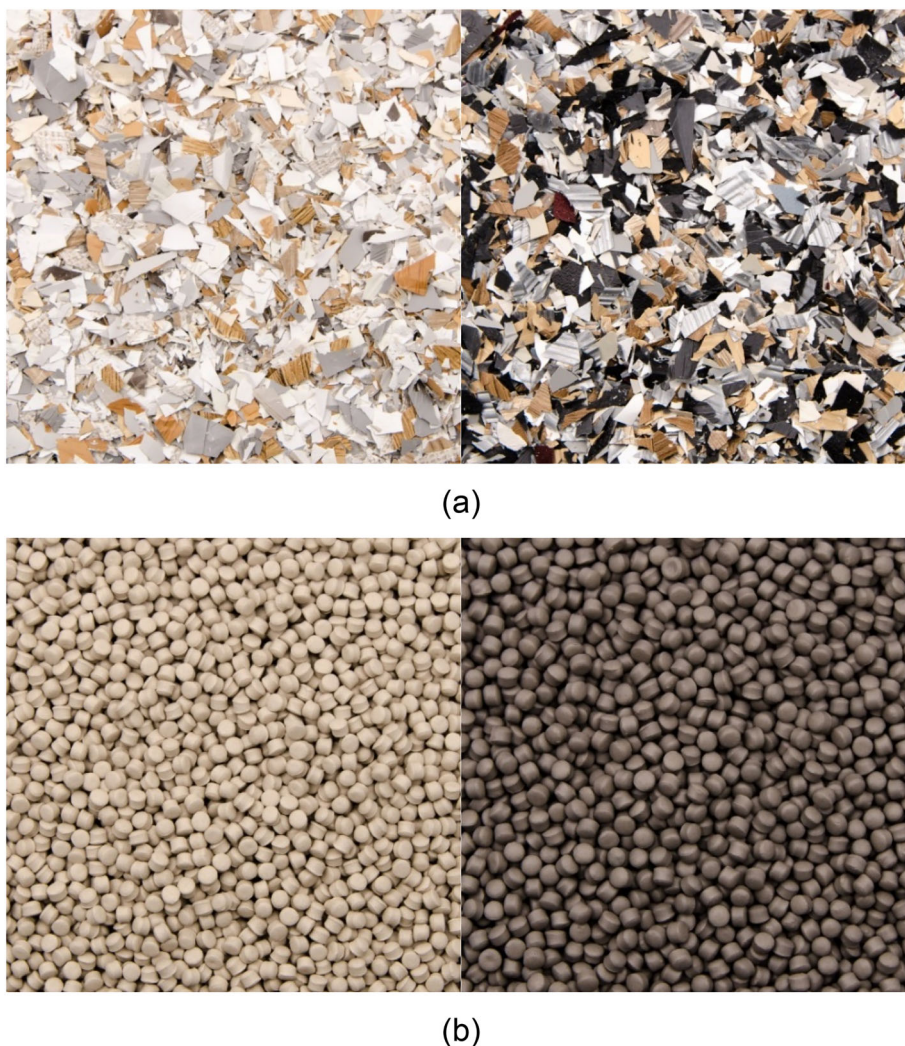
This study aims to investigate the intricate relationships between the key parameters of the extrusion process in mechanical recycling and the property profile of the resulting recyclate. Specifically, it examines the processing of a waste stream primarily composed of polypropylene (PP) originating from a post-industrial source. Moreover, this research investigates the influence of input material variability, considering its role in process fluctuations and its effects on selected recyclate properties. To achieve these objectives, a two-part experimental approach was adopted. In Part A, the process was carried out under controlled conditions, while in Part B, various process configurations, including adjustments to screw speed, filtration setup, and degassing setup, were systematically considered. Subsequently, the study evaluated the effect of these processing conditions on properties such as melt properties, thermal stability, mechanical properties, degassing performance, and the levels of residual volatile organic compounds (VOCs) in the recyclate.

2 | MATERIALS AND METHODS

2.1 | Investigated material

The study investigated the recycling potential of a waste stream originating from post-industrial sources, consisting of pigmented multilayer films. The input materials were delivered in form of flakes with a flake size ranging from 2 to 10 mm. Furthermore, the materials displayed a broad spectrum of colors spanning from white and light gray to dark brown and black. Consequently, after processing, the resulting recyclates exhibited various shades of gray. Figure 1 displays exemplary images of the input materials in flake form along with images of the resulting recyclates showing the two most extreme color cases, light gray and dark gray. These films are primarily tailored for applications related to furniture surfaces and are predominantly composed of PP, with polyethylene (PE) serving as a secondary component. In addition to PP and PE, the material composition includes various additives, lubricants, lacquers, and inks, which enhance the

FIGURE 1 Representative images of (a) the input materials and (b) their resulting recyclates, highlighting the contrast between bright (left) and dark (right) input materials and their influence on the color of their corresponding recyclates. [Color figure can be viewed at [wileyonlinelibrary.com](https://onlinelibrary.wiley.com)]



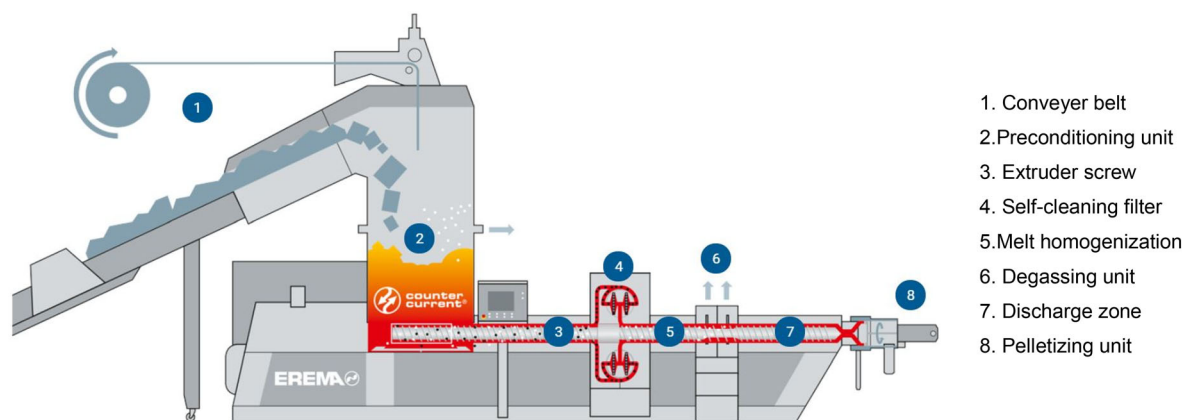
material's durability to withstand certain application-specific loads. This specific composition resulted in a density exceeding 1 g/cm^3 , which is notably higher than that of its main constituents (i.e., PP and PE). Furthermore, the melt mass-flow rate (MFR) of this material measures approximately 4 g/10 min , under test conditions involving a temperature of 230°C and a weight load of 2.16 kg .

2.2 | Material processing

2.2.1 | Regranulation process

Since the materials were received in the form of flakes, the influence of the preparatory stage was not considered in the present study. Therefore, this investigation focused solely on the regranulation stage in the recycling process. Materials were converted to recyclates in the form of pellets using an INTAREMA 1108TVEplus recycling extrusion system from EREMA Group (Ansfelden, Austria). A schematic illustration of the regranulation process is depicted in Figure 2.

The regranulation process starts with an automatic conveyor belt, which directly feeds the input materials (i.e., flakes) from the big bags (BBs) into a preconditioning unit (PCU). The PCU, where the initial degassing occurs, serves as the first homogenizing step, involving mixing, drying, and pre-compacting of the material before it enters the melt extrusion step. Following this, the material is conveyed through an automatic slider into the extruder, which is equipped with both melt filtration and degassing units. At the end of the first screw section, the melt temporarily exits the extruder barrel to pass through the melt filtration unit, in which screen disks collect contaminants as the polymer melt flow through. The self-cleaning mechanism of the filter is guaranteed by scrapers removing the contaminants from the screen disks and directing them to a discharge system. Subsequently, the melt reenters the extruder barrel to pass through the degassing unit for potentially removing the emissive volatiles from the melt. Afterward, the melt is conveyed through the pelletizing unit to form and cool down pellets. Finally, the pellets are transported into a



1. Conveyer belt
2. Preconditioning unit
3. Extruder screw
4. Self-cleaning filter
5. Melt homogenization
6. Degassing unit
7. Discharge zone
8. Pelletizing unit

FIGURE 2 Schematic illustration of the used recycling extrusion system INTAREMA 1108TVEPlus provided by EREMA Group.¹⁸ [Color figure can be viewed at wileyonlinelibrary.com]

TABLE 1 Summary of the various machine setups and configurations used in this study.

Machine setups	Configuration 1	Configuration 2
Screw speed	150 rpm	250 rpm
Mesh size of the filtration screen	130 to 150 μm	90 to 110 μm
Degassing setup	Vacuum	Atmospheric

centrifugal drum, which serves as a drying mechanism. This drum is coupled with a paddle wheel that transports the resulting recyclates to a balance, marking the completion of the regranulation process.

2.2.2 | Experimental design space

To cover a broad range of processing setups (PSUs), the experimental design space was divided into two parts, in which the settings of the recycling extruder were either kept constant (Part A) or systematically varied (Part B). The aim of the former was to assess the variability of the input material, and therefore feedstock, by analyzing the behavior of recyclate properties over time. To this end, the recycling extruder was operated at a constant screw speed of 230 rpm for 5 h with an average throughput of roughly 510 kg/h. Moreover, a filtration setup with a mesh size from 90 to 110 μm was used for this PSU.

In contrast, the intention of Part B was to systematically assess the influence of selected processing conditions on recyclate properties. Tables 1 and 2, respectively, provide a summary of the machine configurations as well as experimental processing conditions and present a tabulated list of the resulting combinations of PSU. The machine setups include: (i) the screw speed, (ii) the mesh size of the filtration screen, and (iii) the degassing setup.

For each of these, two different configurations were examined, yielding a total number of eight PSUs. Note that atmospheric degassing was achieved by turning off the vacuum pump of the degassing zone. Each PSU was kept constant for 45 min.

2.3 | Characterization techniques

2.3.1 | Sampling and sample preparation

Materials were distributed across 10 BBs, each containing approximately 850 kg of material, accounting for a total of around 8.5 metric tons of the specific post-industrial waste materials. The first three BBs were designated for Part A of the study, while the remaining bags were allocated for Part B. To obtain representative samples from the input material stream, position-based stratified random sampling, as proposed by Akhras and Fischer,¹⁹ was employed for the sample collection from each BB. Thereby, each BB was subdivided into three distinct strata (bottom, middle, top), from which three increment samples were collected. Subsequently, the increment samples were mixed to create composite samples that are presumably representative of the respective BBs. These composite samples were then used for the analysis of the input materials.

A time-based sampling approach was employed at the discharge end of the extrusion line, particularly after the centrifugal drum, to collect samples of the resulting dried recyclates. In the case of Part A of the experimental design space, samples were collected at intervals of 30 min, considering the residence time in the PCU of approximately 30 min. On the other hand, concerning Part B of the experimental design space, the processing time for each PSU was set to 45 min. Here, a total of

TABLE 2 List of the experimental matrix for Part B of the experimental design space based on the various processing setups.

Processing setup (PSU)	Screw speed [rpm]	Filtration setup–Mesh size range [μm]	Degassing setup [–]
PSU1	150	F100 (90/110)	Vacuum
PSU2	250	F100 (90/110)	Vacuum
PSU3	150	F100 (90/110)	Atmospheric
PSU4	250	F100 (90/110)	Atmospheric
PSU5	150	F140 (130/150)	Vacuum
PSU6	250	F140 (130/150)	Vacuum
PSU7	150	F140 (130/150)	Atmospheric
PSU8	250	F140 (130/150)	Atmospheric

three samples were collected for each PSU, with one sample obtained every 15 min, covering the beginning, the middle, and the end.

In terms of the sample preparation, following a size distribution analysis conducted only on selected samples, the individual composite samples from the BBs underwent an additional size reduction step by a Retsch SM 300 cutting mill (Retsch GmbH, Haan, Germany) operating with a rotor speed of 1200 rpm. This step aimed to enhance the homogeneity of the input materials, leading to samples with a maximum particle size of 4 mm. Subsequently, the milled materials, along with the recyclates, were then directly subjected to measurements where no further processing was required, such as MFR.

For other measurements that require the preparation of specific test specimens, for instance tensile and impact specimens, further processing was necessary. Direct processing of the input materials was unfeasible due to the vast amounts of emissive volatiles detected in the input stream. These volatiles hindered the production of such specimens of the input materials since the volatiles were intensively released once the material was in the melt state. Therefore, the analysis of the input materials was limited to measurements that did not require any further processing as the production of the necessary specimens was not feasible without being subjected to an effective degassing mechanism.

On the other hand, in the case of the resulting recyclates, given that PP is the predominant component in the material composition, the processing technology and parameters were determined in accordance with the standard ISO 19069-2.²⁰ Multipurpose specimens (MPSs) of type A1 were injection-molded using a Victory 60 injection molding machine featured with a 25 mm barrel (Engel Austria GmbH, Schwertberg, Austria), following ISO 3167 and ISO 294-1.^{21,22} As the MFR of the material was known to fall within the range of 1.5–7 g/10 min, the processing temperature (i.e., melt temperature) was set to 235°C, in line with the recommendations of ISO 19069-2.²⁰ Similarly, type 1 specimens for Charpy impact tests, as specified in ISO 179-1,²³ were also injection-

molded in accordance with the same standards. Prior to testing, all injection-molded specimens were preconditioned for 3 up to 5 days at room temperature (i.e., 23°C) and 50% relative humidity as recommended in ISO 291.²⁴ Moreover, to ensure a high level of homogeneity, other measurements were also performed on the cross section of MPSs and not on the recyclates.

2.3.2 | Melt mass-flow rate

To evaluate the processability of the materials, MFR measurements were performed on samples of the input stream (i.e., flakes) as well as on the resulting recyclates from the various PSUs. Additionally, the measurements were also performed to determine the influence of the various processing parameters on the flowability of the material, hence estimating the processing-induced degradation. Measurements were carried out using an Aflow extrusion plastometer instrument (ZwickRoell Group, Ulm, Germany). To ensure a good representation of the material property, three measurements of each sample were performed. Each sample, weighing approximately 4 g, was subjected to the displacement-measurement method (method B) as outlined in the standard ISO 1133-1.²⁵ Given that the input material is PP-based, the test temperature was set to 230°C. After loading the cylinder and preheating for 300 s, the material was automatically compressed by a piston under a load of 2.16 kg to flow through a die with a nominal height of 8 mm and a diameter of 2.095 mm. For each measurement, six extrudates were cut and weighed to calculate the MFR values based on the vertical displacement of the piston.

2.3.3 | Thermal analysis

Determination of the ash content

Since the investigated materials were known to contain various additives and fillers, ash content (AC) tests were

conducted to detect the levels of inorganic residues within this specific waste stream. In the plastics recycling sector, AC is commonly used due to the potential fluctuations in inorganic residue levels in recycled plastics, which can be attributed to variations in the input material. Such residues can significantly affect the mechanical properties of the resulting recyclates, depending on their size, content, and dispersion within the polymer matrix. Therefore, it is essential to identify and quantify these residues as they can have a notable impact on the material properties.^{26,27}

In this study, AC was determined for both the input materials as well as the output (i.e., the recyclates) of Part A and Part B. The test procedure followed method A for rapid ashing, as outlined in the ISO 3451-1 standard.²⁸ Ashing was carried out using quartz fiber crucibles in a Phoenix microwave muffle furnace (CEM Corporation, North Carolina, USA). Samples of approximately 4 ± 0.2 g of each material were tested. The test portions were directly subjected to calcination in the microwave furnace at a temperature of 750°C for a duration of 15 min. Subsequently, the crucibles were weighed, and the AC values were determined using Equation (1). To ensure a good level of accuracy, four samples of each material were tested, and then the mean values and the standard deviations (SDs) were calculated accordingly.

$$A\% = \frac{m_1 - m_c}{m_0} \times 100, \quad (1)$$

where $A\%$ is the inorganic residues (i.e., AC), m_0 corresponds to the initial mass of the test portion, m_c is the measured mass of the crucible, and m_1 is the measured mass of the crucible including the obtained ash.

Determination of the thermal stability

To assess the thermal stability and the resistance to oxidative decomposition of the materials, the oxidation induction temperature (dynamic OIT) was measured using a differential scanning calorimeter DSC 4000 (PerkinElmer Inc., Waltham, MA, USA). The production of appropriate homogeneous specimens (e.g., MPS) of the input materials, from which samples for the dynamic OIT measurements can be extracted, was unfeasible due to the significant presence of emissive volatiles in the input stream. Nonetheless, dynamic OIT measurements typically serve as an indication of the thermal stability of a material and its resistance to oxidation. Therefore, dynamic OIT measurements were exclusively performed on the recyclates post the extrusion process to assess the influence of the various processing conditions on the material. Samples of approximately 8 ± 1 mg each were cut from the cross-section of the injection molded

MPS. Three samples of each material were encapsulated in perforated aluminum pans. A dynamic temperature scan program was defined for the measurement, starting with an initial isotherm at 30°C for 1 min, followed by a gradual increase in temperature with a constant heating rate of 10 K/min up to 260°C. Synthetic air was utilized as purge gas, flowing constantly into the measurement compartment at a rate of 20 mL/min. To ensure the accuracy of the evaluation, the heat flux of the measurements was normalized by the individual sample masses, thus the normalized thermograms were used for the data evaluation. Thereafter, dynamic OIT was determined as the point of interception between the two tangents at the onset of exothermic oxidation on the thermogram. The measurements and subsequent data evaluation of the dynamic OIT were conducted in accordance with standards ISO 11357-1 and -6.^{29,30}

2.3.4 | Mechanical tests

Tensile tests

Monitoring the tensile properties of the recyclates after undergoing different processing conditions was of interest in this study. To ensure a good representation of the influence of the processing conditions, two samples of each PSU were considered in this evaluation. Thereafter, 10 injection-molded MPS of each sample were subjected to tensile testing using a universal testing machine Zwick/Roell AllroundLine Z005 equipped with a multiXtens strain measurement system (ZwickRoell Group, Ulm, Germany). The test parameters were set according to ISO 527-1 and -2^{31,32} with a transverse speed of 1 mm/min for the determination of the tensile modulus until a strain of 0.25% is reached. Afterwards, the speed is increased automatically to 50 mm/min and kept constant until failure.

Charpy notched impact tests

To gain a more comprehensive overview of the influence of processing on the mechanical properties of the materials, Charpy notched impact strength (NIS) of the resulting recyclates was also measured. Tests were performed on the injection molded type 1 impact specimens using a non-instrumented HIT25P pendulum impact tester (ZwickRoell Group, Ulm, Germany). Prior to testing, a type A V-shaped notch ($45^\circ \pm 1^\circ$ notch angle, 0.25 ± 0.05 mm notch tip radius), as depicted in ISO 179-1,²³ was introduced into the specimens using an RM2265 automatic rotary microtome (Leica Biosystems Nussloch GmbH, Nussloch, Germany). Similar to the tensile tests, a set of 10 conditioned notched specimens of each sample were tested. Tests were carried out edgewise, following the prescribed procedure in ISO 179-1.²³

2.3.5 | Analysis of volatile organic compounds

Degassing performance

The degassing performance of selected PSUs was qualitatively determined based on the approximation of the degassed fraction (F_d) in the extrusion process. Thus, the concentrations of the VOCs in the relevant input materials and the resulting recyclates from the specific PSUs were experimentally determined using a vacuum oven (Binder Energietechnik GmbH, Baernbach, Austria). Thereafter, F_d of the desired PSUs was determined according to Equation (2), where C_{in} and C_{out} denote the experimentally measured VOC concentrations of the input and the output materials of the extrusion process (i.e., flakes and recyclates), respectively.

$$F_d = \frac{C_{in} - C_{out}}{C_{in}} \times 100. \quad (2)$$

Five measurements were performed for each PSU using samples of around 10 g from the input and the output materials to calculate the mean F_d . The measurements were conducted at 200°C, the maximum temperature attainable on the vacuum oven. Given that this temperature is lower than that in the degassing zone, which is around 220°C, the measurements were extended overnight for approximately 16 h to ensure the complete removal of all volatiles from the polymer. While this approach can be promising for rapid and convenient qualitative comparisons, it is important to note that precisely matching the samples of the input material to those of the output recyclates can be highly challenging. When processing plastic waste in mechanical recycling processes, considerable fluctuations in the input materials are commonly encountered. Hence, proper identification and allocation of input to output samples become crucial. Therefore, this technique is primarily recommended for qualitative comparisons between different processing points, unless the feedstock remains consistent.

Gas chromatography–mass spectrometry

A semi-quantitative analysis of the residual VOC levels in the resulting recyclates was conducted using a Clarus 690 SQ 8 gas chromatograph coupled with a mass spectrometer (GC–MS) (PerkinElmer Inc., Waltham, MA, USA). The instrument was also equipped with a TurboMatrix 650 automated thermal desorption unit (ATD) also from PerkinElmer Inc. The GC system utilized a non-polar HP Ultra 2 separation column (Agilent Technologies, Santa Clara, CA, USA) and the analysis was performed with a flow of helium gas. As mentioned before, the production of suitable homogeneous specimens (e.g., MPS) of

the input materials was not feasible. Consequently, only the output materials (i.e., recyclates) of both Part A and Part B of the experimental design were considered for this analysis. Samples with dimensions of approximately $(2.3 \times 2.5 \times 10.0) \pm 0.3$ mm were cut from the cross-section of the MPSs. To extract the VOCs from the solid polymer matrix, the samples were heated in the ATD to 90°C for 30 min. VOCs were transferred to a cold trap via a continuous flow of helium gas. After the cold trap was rapidly heated, the subsequent separation of the VOCs in the GC was facilitated by employing a temperature program and parameters as outlined in Table 3. To obtain the semi-quantitative results, a one-point calibration reference was conducted prior to the measurements. A solution of 0.5 mg/mL toluene in methanol was analyzed, and the solution was loaded onto a sample tube filled with Tenax TA via a heated packed column injector set at 430°C. The column was purged with helium at a flow rate of 20 mL/min for 30 min, followed by desorption at 280°C for another 30 min. This calibration process was used to establish a response factor (Rf), which represents the ratio between the mass of toluene (m_{ref}) in micrograms (μg) and the corresponding peak area (A_{ref}) as described in Equation (3).

$$\text{Rf} = \frac{m_{ref}}{A_{ref}} \times 10^6. \quad (3)$$

Furthermore, the semi-quantitative VOC levels in $\mu\text{g/g}$ were determined by multiplying Rf by the ratio of the peak area of the sample (A_s) to the sample mass (m_s) in milligrams (mg) as outlined in Equation (4). The VOC level was determined in two distinct samples for each PSU, both constant and variable, and the highest value was considered as the VOC value for that point.

$$\text{VOC} = \text{Rf} \times \frac{A_s}{m_s} \times 10^{-3}. \quad (4)$$

A summary of the various test techniques employed in this study is provided in Table 4, outlining the corresponding test parameters and the used standard methods.

3 | RESULTS AND DISCUSSION

3.1 | Assessment of the input materials

Processing the input materials without employing advanced filtration and degassing systems was not possible. This limitation primarily stemmed from the intricate material composition and the presence of high levels of volatile emissions, which were triggered by elevated

TABLE 3 Summary of the temperature program and parameters of the automated thermal desorption unit (ATD) and gas chromatograph coupled with a mass spectrometer (GC-MS).

ATD parameters		GC-MS parameters	
Mode	2 stage desorption	Transfer line temperature to MSD*/°C	280
Column flow [mL/min]	2.0	Mass range of scan mode/amu	29–450
Desorption flow [mL/min]	40	Solvent delay/min	2
Inlet split flow [mL/min]	44	Temperature program	
Outlet split flow [mL/min]	19	Start temperature	40°C, 2 min
Desorption temperature [°C]	90	Ramp 1	3 to 92°C/min
Desorption time [min]	30	Ramp 2	5 to 160°C/min
Trap temperature [°C]	–30 to 280	Ramp 3	10 to 280°C/min
Heating rate [K/s]	99	End temperature	280°C, 10 min
Trap hold [min]	20		
Valve temperature [°C]	280		
Transfer line temperature [°C]	290		

*Mass-selective detector.

TABLE 4 Overview of the applied test methods on the investigated materials.

Test method	Test conditions		Materials		
	Standard method	No. of measurements	Input	Output (const. PSU)	Output (var. PSU)
Processability					
Melt mass-flow rate	ISO 01133–1, method B	Min. 2, ca. 4 g	x	x	x
Thermal analysis					
Ash content	ISO 3451-1, method A	4, ca. 4 g	x	x	x
Oxidation induction temperature	ISO 11357-1, –6	3, 8 ± 1 mg			x
Mechanical tests					
Tensile tests	ISO 527-1	10 tests, MPS		x	x
Charpy NIS	ISO 179-1, edgewise	10 tests, type 1 specimens			x
Analysis of volatile organic compounds					
Degassing performance	Qualitative analysis	5, ca. 10 g			x
Gas chromatography–mass spectrometry	Semi-quantitative	2, cut from MPS		x	x

processing temperatures once the input material reached the melt state. The extensive release of these volatiles can be attributed to the thermo-oxidative degradation of the individual components, such as lubricants, lacquers, and adhesives, all of which are present in the material's composition. Consequently, the assessment of the input materials was limited to basic characteristics, focusing on aspects involving the material's processability and the residual levels of inorganic residues.

Prior to the preparatory steps for the material analysis, simple size distribution analysis was conducted on the composite samples in flake form of selected BBs. This analysis was carried out using an automatic vibratory sieve shaker.

The results revealed that the majority of the flakes fell within the size range from 2 to 8 mm in at least two dimensions, with only minor fractions deviating from this specific range. Subsequently, the composite samples of all BBs underwent a milling step to reduce the nominal flake size, aiming to enhance the uniformity of the input materials. The milled samples were then used for the subsequent analyzes, which aimed to gain insights into the variability within the input stream.

Figure 3 presents the results of the MFR and the AC measurements obtained from the composite samples collected from the various BBs of the input stream used for this study. As shown in Figure 3a, BB10 exhibited the highest MFR followed by BB3, measuring 4.3 and

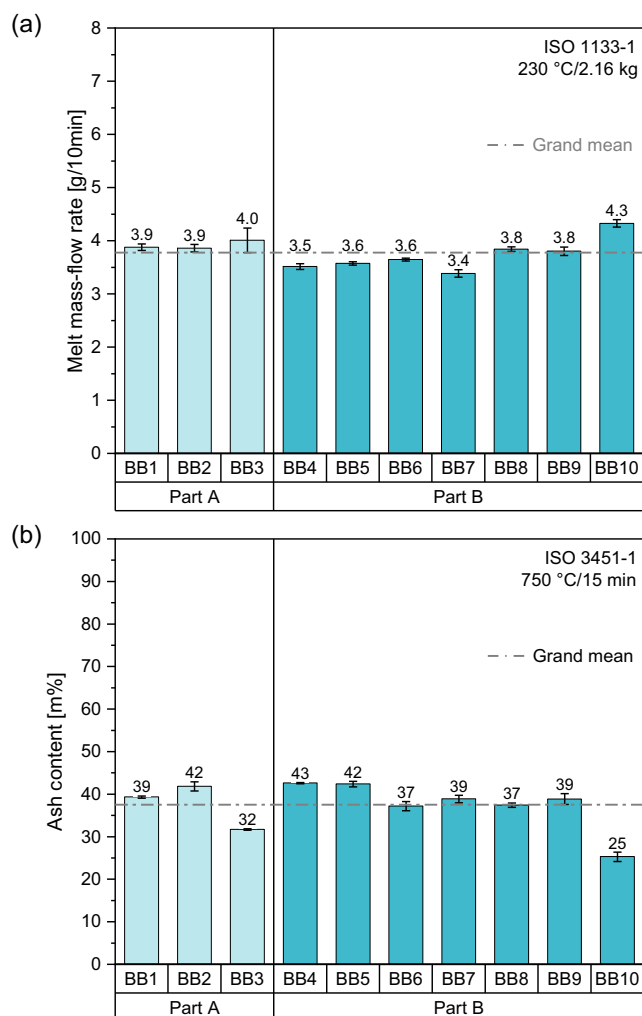


FIGURE 3 Variability level in the properties of the input materials shown by their experimentally measured (a) melt mass-flow rates, and (b) ash content levels across the various big bags (BBs). [Color figure can be viewed at [wileyonlinelibrary.com](https://onlinelibrary.wiley.com/doi/10.1002/app.55731)]

4 g/10 min, respectively. Conversely, MFR of BB7 was the lowest among all with 3.4 g/10 min followed by 3.5 g/10 min for BB4. It is evident that only marginal deviations were observed in the MFR values across all BBs, averaging with a grand mean (GM) of around 3.8 g/10 min. Moreover, when calculating the mean absolute deviation (MAD) for this dataset as expressed in Equation (5), we find that it amounts to only 0.2 g/10 min, indicating roughly a 5% deviation from the GM. Therefore, the MFR values of the input materials show consistency and relatively low variability.

$$\text{MAD} = \frac{\sum |x_i - \bar{x}|}{n}, \quad (5)$$

where x_i is the mean value of the individual BBs, \bar{x} is the GM of the entire dataset, and n is the total number of BBs.

On the other hand, Figure 3b illustrates the AC levels, representing the residual inorganic contents in the input materials. The AC test is a mass-based analysis rather than volume-based. Therefore, the presence of different fillers and pigments with varying densities in a material composition may influence the AC levels in an input stream but cannot give any information about the volume fraction of the fillers and pigments. For instance, fillers like carbon black have a density of approximately 1.8–2 g/cm³,³³ whereas the density of a filler like calcium carbonate is around 2.7 g/cm³.³⁴ These fillers are typically added to enhance the material's durability and mechanical properties, as well as for their coloring function.^{33–35}

In general, the investigated input materials exhibited relatively high AC values, averaging approximately 38 mass% (m%). This can be attributed to the substantial presence of inorganic fillers in the material composition, such as talc, carbon black, and calcium carbonate. Among the 10 BBs, samples of BB4 exhibited the highest AC reaching 43 m%, followed by BB2 and BB5 both at 42 m%. In contrast, BB3 and BB10 samples displayed the lowest AC levels, measuring 32 and 25 m%, respectively. This explains the slightly higher MFR of these two BBs as, among various factors, the viscosity in PP typically increases with increasing the inorganic filler content, and conversely, decreases when the inorganic filler content is reduced.^{36,37} AC levels for the other BBs fell within the range of the overall input stream's GM, that is, 38 m%. These variations can be attributed to the uneven distribution of incorporated fillers and pigments in the input stream, as evident from the flake colors shown in Figure 1. However, the entire dataset has an MAD of 3.7 m%, falling within a 10% range from the GM, which is regarded as an acceptable dispersion. Consequently, the available data, of both MFR and AC measurements, suggest that the variability level within the input materials can be considered relatively low.

3.2 | Assessment of recyclate properties with constant processing conditions

To further investigate the variability within feedstock, the input materials underwent the extrusion process using a constant PSU, whereby all processing parameters were maintained constant for a duration of 5 h. As indicated in Figure 3, three BBs were utilized for this part of the experimental design, exceeding a total of 2.5 tons of input materials. As previously explained in Section 2.2.1, at the discharge end of the processing line, samples of the recyclates were systematically collected at 30-min intervals over the course of the

TABLE 5 Summary of the material data after processing with a constant PSU accompanied by the relevant statistical parameters.

Sampling time [h]	Melt mass-flow rate (MFR) [g/10 min]	Ash content (AC) [m%]	Tensile modulus [MPa]	Stress at yield [MPa]	Strain at break [%]	Volatile organic compounds (VOC) [$\mu\text{g/g}$]
0.5	4.9	35.8	2240	20.9	19.0	
1.0	4.9	34.6	2186	21.1	19.9	79.1
1.5	5.0	37.6	2292	20.6	19.6	
2.0	5.0	40.7	2406	20.1	17.5	83.5
2.5	5.0	42.1	2429	19.6	18.3	
3.0	5.0	40.5	2389	20.3	18.4	82.3
3.5	4.6	36.5	2335	21.7	18.8	
4.0	4.6	36.6	2330	21.8	20.0	70.7
4.5	4.5	32.4	2266	22.9	20.2	
GM	4.8	37.4	2319	21.0	19.1	78.9
SD	0.2	3.1	80.9	1.0	0.9	5.8
MAD	0.2	2.5	65.1	0.8	0.7	4.1
MAD%	3.7%	2.8%	3.9%	4.0%	5.2%	6.6%

extrusion tests in Part A. Subsequently, the obtained samples were subjected to a series of characterization methods including MFR, AC, tensile tests, and ATD-GC-MS analysis. The primary aim of this approach was to assess the variations in the overall property profile of the investigated input material streams after processing, and thus the feedstock variability. The material data obtained from these test methods are compiled in Table 5, along with essential statistical parameters, including GM, SD, and MAD.

Evidently, MAD values for all datasets remained rather low with a divergence below 5% from their respective GMs, except for the datasets related to strain at break and VOC, where the MAD values were slightly higher at 5.2% and 6.6%, respectively. This indicates that, although a certain degree of variation still exists in the datasets of the inspected properties, the data points exhibit a consistent pattern with relatively minimal fluctuations around the mean. Hence, this suggests a moderately low degree of variability in the material.

Additionally, control charts, also known as statistical process control charts (SPCC), were generated to visually monitor the material's performance over the defined processing timeframe. This tool is typically employed to identify existing trends, variations, or anomalies within a dataset, thereby providing a visual representation of changes in the specified properties and an approximation of their level of variability.^{38,39} The corresponding GMs were used as centerlines in the relevant SPCC of each property, while the upper control limits (UCLs) and the lower control limit (LCLs) were calculated based on

the respective SD values of each dataset according to Equations (6) and (7), respectively:

$$\text{UCL} = \bar{x} + (L \times \sigma), \quad (6)$$

$$\text{LCL} = \bar{x} - (L \times \sigma), \quad (7)$$

where \bar{x} represents the GM, σ denotes the SD of each dataset, and L signifies the control limit, which is typically set to 1, 2, or 3.

Figure 4 illustrates the SPCC of the various material properties. Two sets of control limits were considered for this analysis, particularly 1σ and 2σ as all data points fell within these ranges. Consequently, there was no need for a broader control window as 100% conformity was exhibited by the data points. In general, all datasets demonstrate a consistent distribution of the data points around the centerlines, with only minimal discrepancy. These discrepancies can be attributed to common-cause variations that are inherently present in any process,³⁹ especially in the context of plastics recycling. Hence, this further fortifies the notion of the comparatively low degree of variability induced by the input material or the process.

Furthermore, a comparison between the data from the input stream and the corresponding recyclates reveals further insights. In the case of MFR, a noticeable increase was observed after processing. This is demonstrated by the difference between the two GM values, indicating that, on average, the MFR values of the recyclates are approximately 20% higher than those of the input

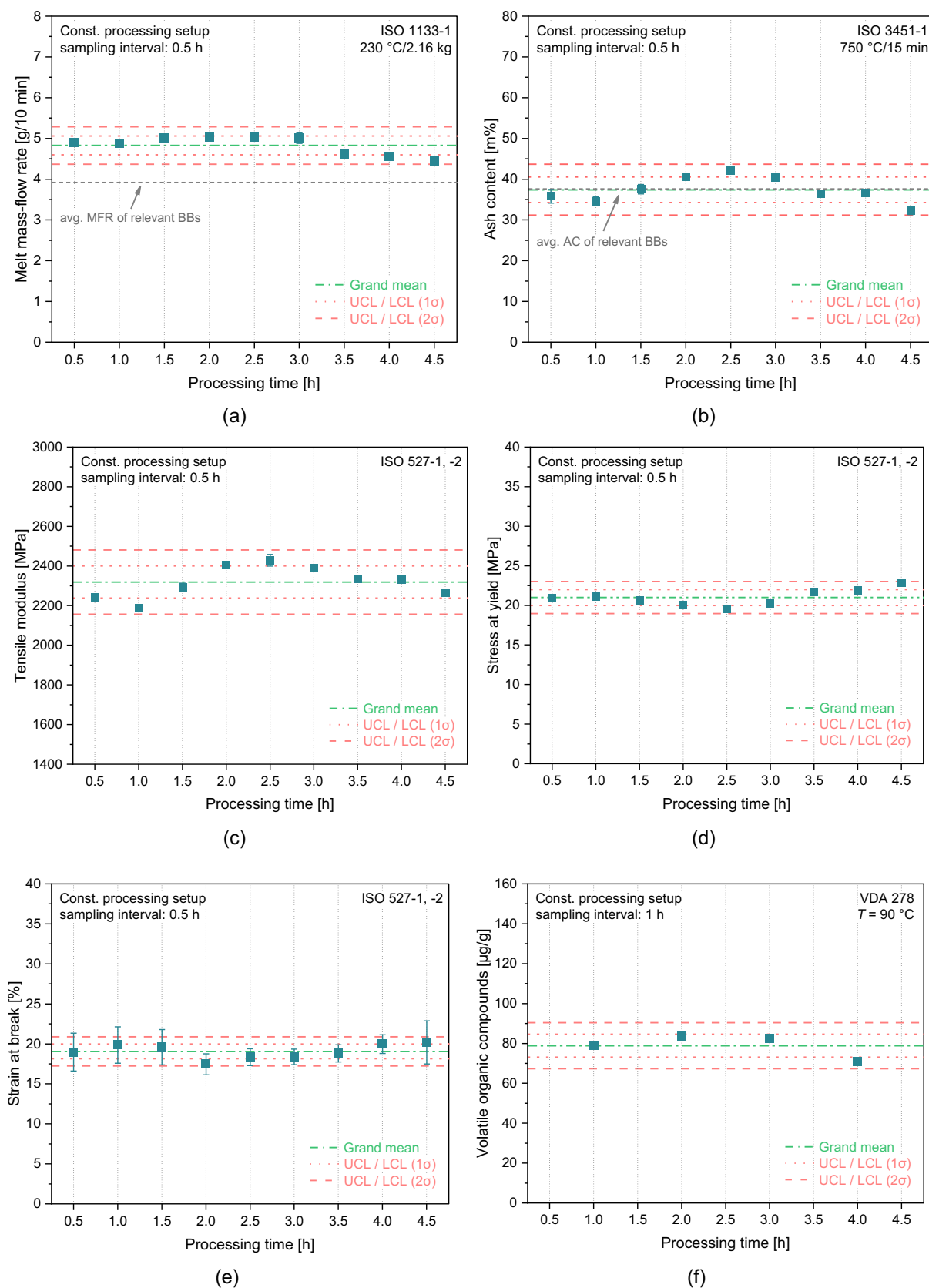


FIGURE 4 Statistical process control charts together with the grand mean, upper control limit (UCL), and lower control limit (LCL), for the key properties of the resulting recyclates including (a) melt mass-flow rate, (b) ash content, (c) tensile modulus, (d) stress at yield, (e) strain at break, (f) volatile organic compounds, following the regranulation process with constant process setups over a period of 5 h. [Color figure can be viewed at [wileyonlinelibrary.com](https://onlinelibrary.wiley.com)]

materials, as shown in Figure 4a. Alterations in MFR values typically suggest changes in the molecular structure of the material, as a consequence of degradation processes within the polymer.⁴⁰ In mechanical recycling of polyolefins (POs), such as PE and PP, materials commonly undergo process-induced thermomechanical degradation.^{10,41–43} This phenomenon induces changes in the molecular structure of the polymer, involving chain scission and branching, due to the combined influence of elevated temperatures and mechanical stresses, such as shearing.^{10,44–46}

Despite their similar nature as POs, PP, and PE exhibit distinct reactions to degradation.¹⁰ During processing, the molecular chains of PE tend to undergo concurrent chain scission and side-chain branching,^{47–49} which can eventually lead to crosslinking and an increase in the polymer viscosity.^{50,51} Whereas degradation in PP is primarily dominated by chain scission, resulting in shorter molecular chains and a subsequent reduction in viscosity.^{41,52} The compatibilization of PP/PE blends using interfacially active block copolymers was experimentally examined in.⁵³

Given that PP is the main constituent in the material composition, the general increase in MFR after processing can be attributed to its typical degradation mechanisms, specifically chain scission.^{41,44,52} On the other hand, AC levels in the materials remained unchanged after processing with the constant PSU. This is evident from the clear overlap between the GM of the recyclates and that of the input materials (i.e., the relevant BBs), as depicted in Figure 4b.

3.3 | Assessment of the Recyclate properties with variable processing conditions

3.3.1 | Influence of processing conditions on the melt properties

The second part of the experimental design (Part B) aims to systematically evaluate the influence of predefined processing conditions (Table 2) on the key properties of the resulting recyclates. The assessment encompasses the impact of three critical elements in the mechanical recycling process of thermoplastic waste, including the employed screw speed, filtration setup, and degassing setup. Furthermore, to acquire a deeper understanding of the process, variations in the melt temperature resulting from the different PSUs were also measured using a thermocouple mesh (TCM). The TCM was positioned at the discharge end of the extruder before the granulation unit, including 13 thermocouples systematically distributed

over the circular cross section of the flow channel. While one of these measured the melt temperature in the channel center, the remaining were located at three distinct radial positions, thereby measuring the temperature profile over the cross section. Melt temperature is commonly acknowledged as one of the critical variables in polymer processing, which has a direct impact on the process stability and the quality of the final product.⁵⁴

Figure 5 illustrates the influence of the various PSUs on the mean melt temperature measured (mean of all 13 temperature values), along with the corresponding MFR values of the resulting recyclates. When comparing the mean melt temperature across the different PSUs (Figure 5a), no significant influence from the filtration system nor the degassing method can be observed. However, a clear correlation between the mean melt temperature and the screw speed is obvious, with both parameters increasing concurrently. Increasing the screw speed from 150 to 250 rpm results in rise in the melt temperature on average of 18°C, accounting for approximately 7%. This temperature increase can be attributed to viscous heating, where higher screw speeds induce greater shear forces and thus increased dissipation rates, leading to elevated melt temperatures.⁵⁵

Moreover, it is worth noting that the SD consistently exhibits a higher value at 150 rpm compared to 250 rpm within the individual datasets. This suggests increased variability among the distinct radial positions in the melt flow when operating at the lower screw speed, specifically 150 rpm. Consequently, a clear correlation emerges, indicating that higher screw speeds, such as 250 rpm, contribute to enhancing the thermal homogeneity, which, in turn, leads to a reduction in temperature gradients.⁵⁶ Overall, in the context of this case study, it can be inferred that the primary parameter influencing the melt temperature is the screw speed.

Similar to the findings in Part A, the processing of the input waste stream in Part B also resulted in an overall increase in the MFR values of the resulting recyclates. This trend is illustrated in Figure 5b, where the GM of the MFR values for the recyclates (4.6 g/10 min) exceeded that of the relevant BBs in the input stream (3.7 g/10 min) by over 20%. This general rise in the MFR values can clearly be attributed to the improved material's homogeneity and the conventional thermomechanical degradation mechanisms of the PP fraction within the material. As a result, it can be concluded that the prevailing degradation mechanism in the investigated waste stream was chain scission, primarily due to the dominance of PP in the material composition. This conclusion is corroborated by the consistent increase in the MFR values observed after processing in both parts of the experimental design.

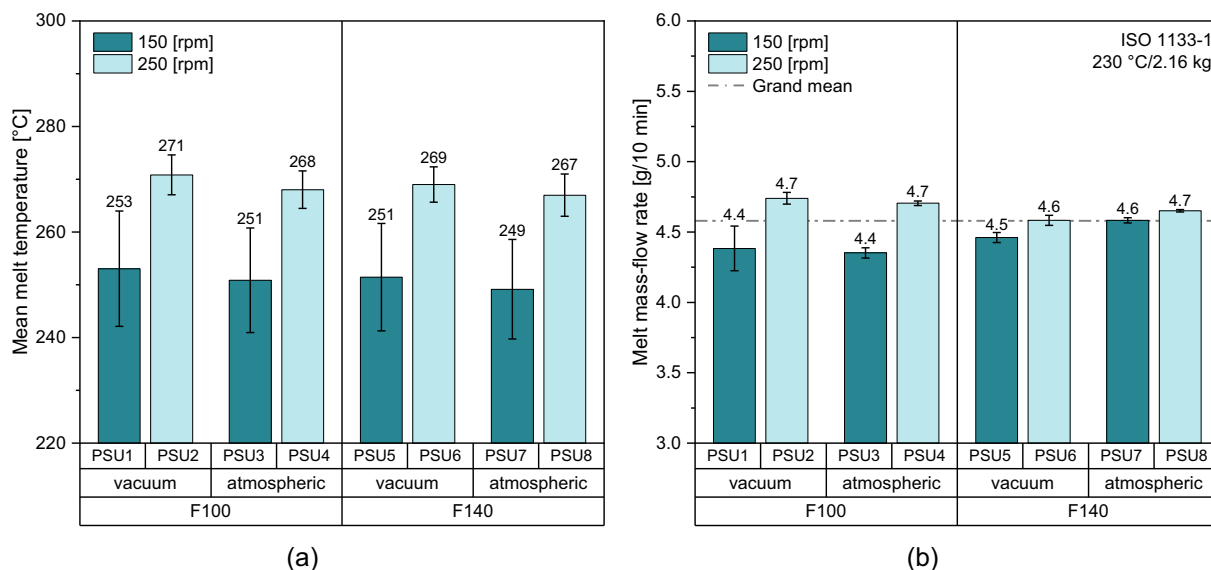


FIGURE 5 Influence of the various process setups (PSU) in the extrusion process—including two different screw speeds (i.e., 150 and 250 rpm), various filtration screen sizes (i.e., F100, F140), and different degassing setups (i.e., vacuum and atmospheric)—on (a) the mean melt temperature, and (b) melt mass-flow rate. [Color figure can be viewed at [wileyonlinelibrary.com](https://onlinelibrary.wiley.com)]

When assessing the effects of the various PSUs on the material's MFR, no influence from either the filtration system or the degassing method can be distinguished. Moreover, similar to the pattern observed in the mean melt temperature, though less pronounced, the MFR increased by up to 6% at the higher screw speed of 250 rpm. This trend can be linked to the elevated melt temperature resulting from the higher screw speed, which in combination with increased shear stresses, may have induced greater degradation within the material. Hence, accounts for the higher MFR values observed in the resulting recyclates.

3.3.2 | Inorganic content and thermal stability

Figure 6 shows the results of the thermal analysis of the resulting recyclates, including AC levels and the dynamic OIT. Similar to the findings of the input materials, AC levels remained relatively high in the recyclates, ranging from as low as 28 m% to as high as 43 m% and averaging around 38 m% (Figure 6a). This consistency can be attributed to the significant presence of inorganic fillers in the material composition of the input stream. While it is evident that a higher degree of variability exists in the AC levels of the recyclates, the GM of the output aligns with that of the relevant BBs in the input stream, which also hovers around 38%.

Upon closer examination of the individual datasets, higher AC levels can be observed at higher screw speeds

under atmospheric degassing. Conversely, no clear trend can be detected under vacuum degassing conditions. This suggests that the deviations in the outcome of this analysis are of a random nature and likely dependent on the variability in the input materials as well as the distribution of the inorganic fillers throughout the entire waste stream. Therefore, considering that no discernible influences from the processing conditions on the AC levels could be detected, it is safe to assume that this property remains unaffected by these specific processing conditions.

Furthermore, the results of the oxidation induction temperature measurements are presented in Figure 6b. This method is typically employed to assess the thermal stability and resistance to oxidation of a material.⁵⁷ In this study, the aim of these measurements was to evaluate the inherent thermal stability of the materials, which is influenced by the effectiveness of the residual stabilizers, and to determine if certain processing conditions induce greater degradation within the polymer. In addition to the thermomechanical degradation, thermo-oxidative degradation also occurs during mechanical processing of plastics due to exposure to oxygen and other contaminants at elevated temperatures.^{43,58} Therefore, to prevent this type of degradation, suitable stabilizer packages are typically introduced into the material during processing.⁵⁹ However, to avoid introducing systematic errors and to ensure unbiased evaluation of this specific waste stream, stabilizer packages were not added during the recycling process within the framework of this case study.

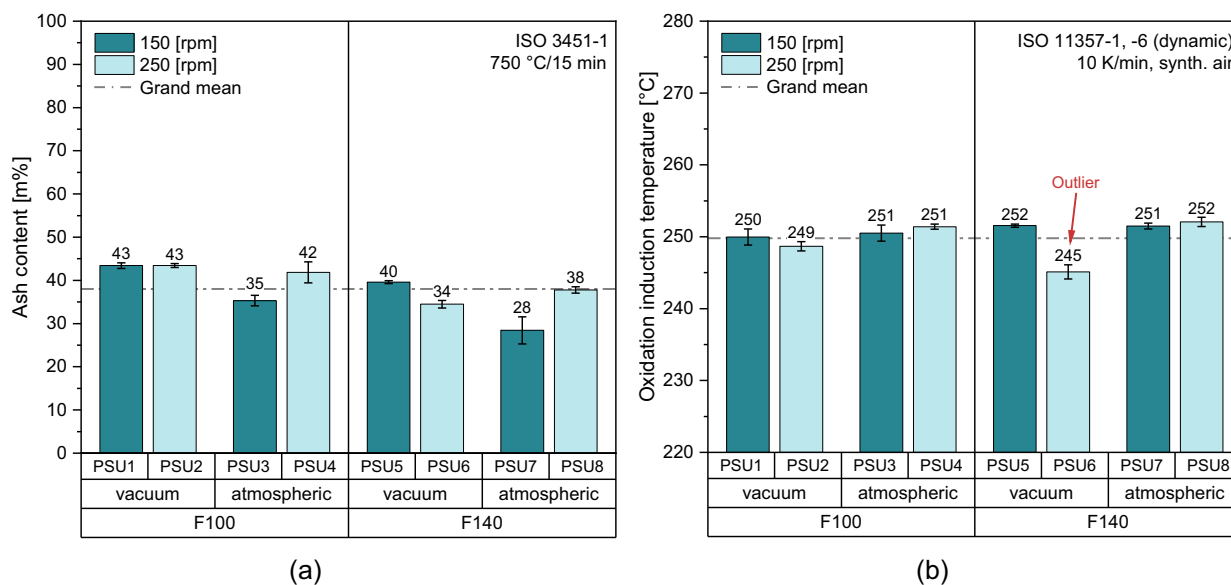


FIGURE 6 Influence of the various processing setups on the inorganic residues in the material and its resistance to oxidation, respectively illustrated by (a) ash content, and (b) oxidation induction temperature (dynamic OIT). [Color figure can be viewed at [wileyonlinelibrary.com](https://onlinelibrary.wiley.com/doi/10.1002/app.55731)]

Evidently, all PSUs yielded comparable dynamic OITs, consistently hovering around $\sim 250^{\circ}\text{C}$, except for one outlier resulting from PSU6 that had a dynamic OIT of 245°C . This slightly lower OIT observed in the recyclate of PSU6 may be attributed to a lower content of residual stabilizer in the material. Nonetheless, a dynamic OIT of approximately 250°C is generally regarded as high for POs, signifying an excellent thermal stability of the resulting recyclates. Although no significant impact from the various PSUs on the dynamic OIT could be detected, it is noteworthy that the overall dynamic OIT values were lower than the mean melt temperature, which averaged 251 and 269°C at 150 and 250 rpm, respectively. Theoretically, this suggests that degradation was initiated during processing, especially at PSUs with higher screw speeds and, consequently, elevated melt temperatures.

3.3.3 | Influence of processing conditions on the mechanical properties

In addition to processability, mechanical properties are vital for determining a material's functionality and overall quality. Alterations during processing, resulting from degradation or changes in molecular structure, often correspond to shifts in mechanical performance. Therefore, assessing the mechanical properties of the recyclates after exposure to various processing conditions was a primary focus in this study. An overview of the investigated mechanical properties is depicted in Figure 7, including the key tensile properties and Charpy NIS.

The tensile modulus values for the resulting recyclates were notably high, averaging around 2340 MPa (Figure 7a). This high stiffness is attributed to the substantial inorganic filler content in the material, which is commonly used to enhance durability against certain application-specific loads.^{33–35,60–62} However, a high degree of variability in the modulus values, ranging from as low as 1944 MPa (PSU7) to as high as 2716 MPa (PSU2), can also be observed, which indicates an impact from the different processing conditions.

Recyclates processed with the coarser filtration system F140, generally, had lower modulus values compared to those processed with the finer filtration system F100. This might be due to larger contaminants escaping the filter and acting as defects in the polymer matrix, thus reducing its stiffness. Furthermore, a clear correlation exists between the tensile modulus and the screw speed, as the higher speed consistently led to higher modulus values, except for an outlier in PSU6. This observation is attributed to the chain scission of the molecular chains of the PP fraction in the material composition, resulting in shorter molecular chains. Consequently, this leads to enhanced mobility of the polymer chains,^{41,52} which facilitates the formation of larger crystalline phases in the polymer, thereby increasing the degree of crystallinity.^{41,43,52,63} This increase in crystallinity corresponds to an increase in the material's stiffness and strength accompanied by a reduction in the material's elongation.⁴¹ Furthermore, as previously demonstrated in Figure 5a, the melt temperature rose proportionally with the screw speed, leading to greater degradation in the polymer melt, which in turn results in higher modulus.

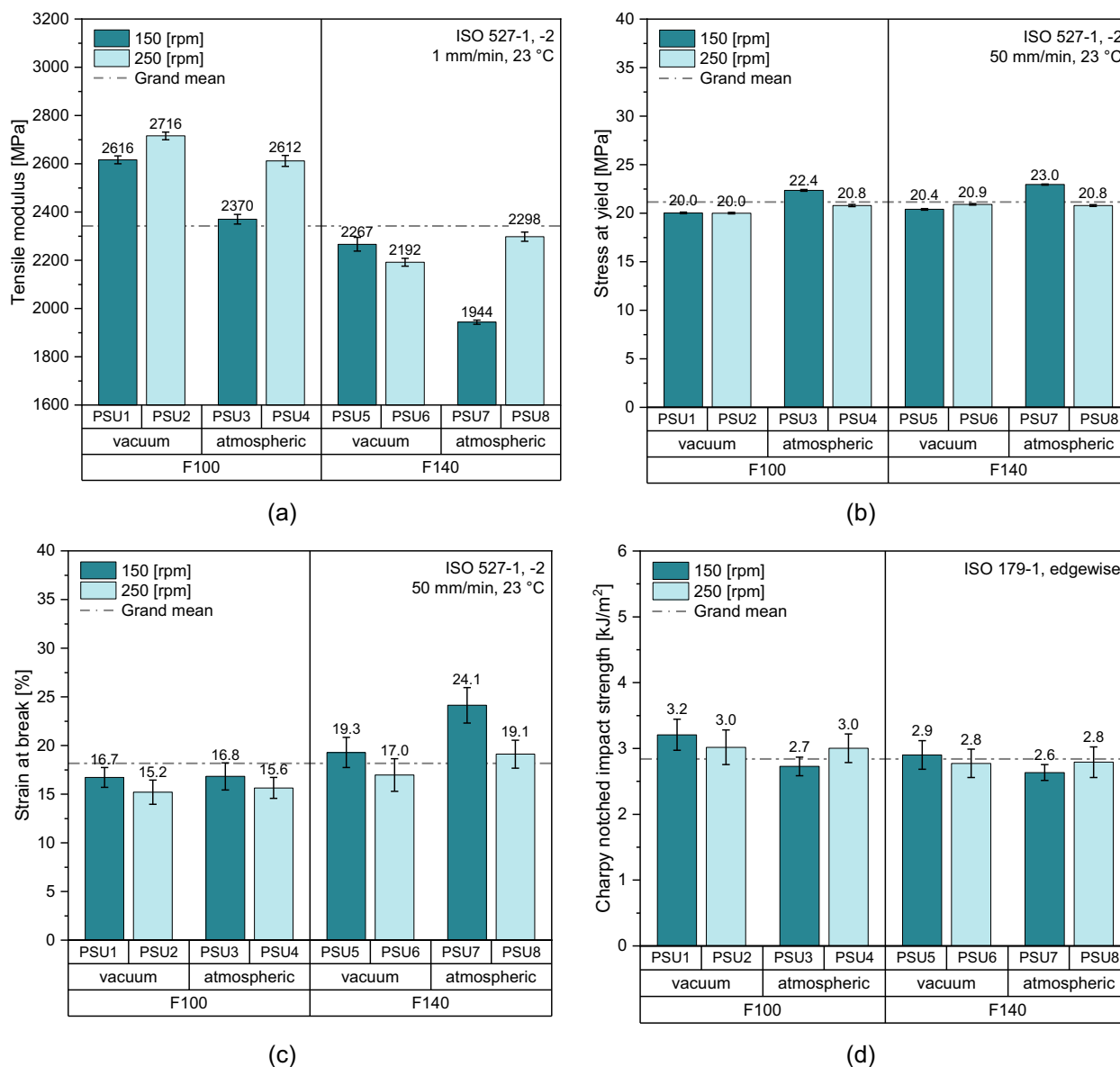


FIGURE 7 Influence of the various process setups (PSU) in the extrusion process on the mechanical properties of the resulting recyclates, demonstrated by (a) tensile modulus, (b) stress at yield, (c) strain at break, and (d) Charpy notched impact strength (Charpy NIS). [Color figure can be viewed at wileyonlinelibrary.com]

Examining the individual datasets of the recyclates processed with the F100 filtration system, that is, PSU1 to PSU4, shows that the higher screw speed led to higher tensile modulus by approximately 4% under the vacuum degassing and about 10% under atmospheric degassing. However, it must be noted that the recyclate of PSU4 had a significantly higher content of inorganic fillers (42 m%), as shown in Figure 6a, compared to that of PSU3 (35 m%). This disparity in the inorganic filler content partially contributed to the increased tensile modulus, in addition to the influence of the higher screw speed. Nevertheless, a difference of approximately 100 MPa is observed between PSU2 and PSU4, which had comparable

inorganic filler contents (~ 42 m%). Hence, this difference can possibly be associated with the different degassing approaches.

When examining the datasets of the other filtration system, PSU7 and PSU8 exhibit the same pattern observed in the F100 datasets, with the tensile modulus of PSU8 exceeding that of PSU7 by more than 350 MPa ($\sim 18\%$). This substantial difference in modulus values can primarily be attributed to the noticeably higher inorganic filler content in the PSU8 recyclate, which amounts to 38 m%, compared to only 28 m% in PSU7 (Figure 6a). Conversely, PSU5 and PSU6 showed the opposite trend, with PSU5 having a 75 MPa ($\sim 3.5\%$) higher modulus,

despite the latter being processed at the higher screw speed. This outlier trend can also be associated with the levels of inorganic fillers present in the respective recyclates, with 40 and 34 m% in PSU5 and PSU6, respectively.

Furthermore, the stress at yield values of the resulting recyclates seem to be consistent, averaging approximately 21 MPa, with no discernible pattern influenced by the varying processing conditions (Figure 7b). However, it is evident that the recyclates resulting from PSU3 and PSU7 had slightly higher stress at yield values, surpassing the GM by approximately 6% and 9%, respectively. The relatively higher stress at yield values can be attributed to the lower levels of inorganic fillers in these specific recyclates.

On the other hand, the strain at break averaged about 18%, with PSU2 recyclate having the lowest value, while the PSU7 recyclate having the highest, with strain values of 15.2% and 24.1%, respectively. The strain at break values exhibited a clear correlation with the screw speed across all datasets. The strain at break value decreased with increasing the screw speed by around 10%. This difference becomes more pronounced, reaching approximately 20%, when comparing the strain values of PSU7 and PSU8. However, this significant decrease can also be directly linked to the substantially higher levels of inorganic filler content in PSU8 in comparison to PSU7, amounting to 38 and 28 m%, respectively.

Finally, Figure 7d presents the Charpy NIS values for the resulting recyclates. It is evident that all recyclates produced under the various processing conditions had comparable, yet relatively low, Charpy NIS values, averaging around 2.8 kJ/m². PSU1 recyclate showed the best performance with a Charpy NIS of 3.2 kJ/m², while the PSU7 recyclate exhibited the worst performance with 2.6 kJ/m². Interestingly, upon the comparison between the individual datasets, Charpy NIS values decreased with the higher screw speed under vacuum degassing but increased under atmospheric degassing, regardless of the employed filtration system. However, due to the consistently low Charpy NIS values and the overlapping SDs of nearly all data points, it can be inferred that the variation in this property is of a random nature. Furthermore, the Charpy NIS values of the investigated materials lie on the lower end of the range observed in some commercial rPP grades. According to Gall et al.,⁶⁴ Charpy NIS values for these grades can range from as low as 2 kJ/m² to as high as 50 kJ/m², depending on the PP type.⁶⁴ Typically, the toughness of a material is influenced by various factors, including the degree of crystallinity⁴¹ as well as the type and size of the inorganic fillers present in the polymer matrix.^{60,61,65} Hence, the relatively low NIS values in this study can generally be attributed to the substantial

presence of the inorganic fillers in the recyclates, combined with the process-induced degradation and thus supposedly increased degree of crystallinity in the PP fraction.

Numerous research studies examined the impact of various aspects, such as size, type, and content, of different inorganic fillers on the mechanical properties of PP.^{60,61,65–67} For instance, Zebarjad et al.⁶⁶ conducted a study to investigate the mechanical properties of PP filled with varying amounts of calcium carbonate, aiming to understand its role in the deformation and fracture behavior of the polymer matrix. Another study by Supaphol et al.,⁶⁵ also examined the influence of calcium carbonate, considering varying contents and particle sizes, on mechanical performance of PP. The former study,⁶⁶ established a clear relationship between filler content and the tensile properties of PP. Their findings indicated that an increase in calcium carbonate content within the polymer led to an increase in tensile modulus while causing a decrease in both stress at yield and strain at break. Similarly, in the study by Supaphol et al.,⁶⁵ a comparable trend was observed in the tensile modulus and stress at yield with increasing filler content. They further elucidated that the reduction in stress at yield was predominantly influenced by the filler content rather than particle size. Furthermore, they also assessed the impact of calcium carbonate on material toughness through Izod impact measurements. Their research demonstrated that impact strength was affected by both particle size and filler content, exhibiting a decrease as these parameters increased. Consequently, it can be concluded that the findings and analysis of the mechanical properties in the current study align with the existing literature.

3.3.4 | Influence of processing conditions on the volatile organic compounds

VOCs represent a critical class of contaminants frequently found in recycled plastics. These contaminants affect the recyclate's quality by, for example, causing undesired odors in the recyclates that could potentially limit their suitability for certain applications.⁶⁸ Therefore, the removal of such contaminants has become increasingly important in recent years to prevent the presence of residual odors in the recyclates. Consequently, the analysis of VOCs has also gained prominence in the field of plastics recycling. This section assesses selected recyclate samples using two test methods to evaluate the effectiveness of the degassing process and measure the remaining VOC levels in the resulting recyclates.

From a processing point of view, the specific type and individual constituents of the VOCs are typically of

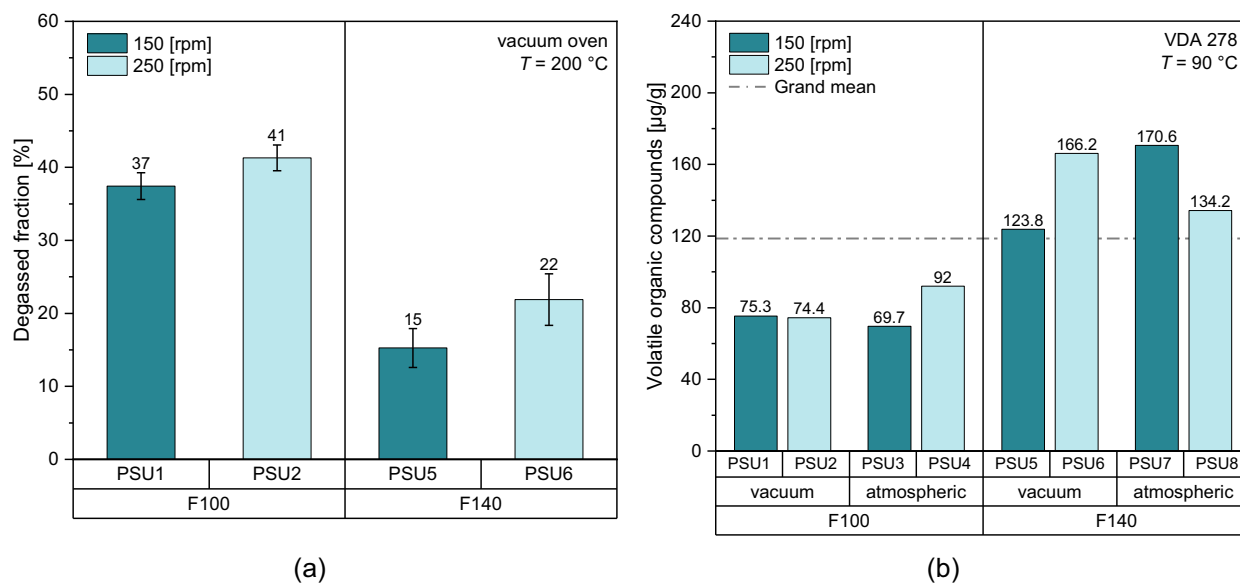


FIGURE 8 Influence of the various process setups (PSU) in the extrusion process on the degassing performance, demonstrated by the (a) degassed fraction, and (b) total volatile organic compound levels present in the recyclates. [Color figure can be viewed at [wileyonlinelibrary.com](https://onlinelibrary.wiley.com/doi/10.1002/app.55731)]

secondary importance. Instead, the primary focus is placed on assessing the total VOC concentration within the polymer. Figure 8a illustrates the levels of the degassed fraction F_d offering an approximation of the degassing performance in the extrusion process. Given that real-life recycling processes typically employ vacuum degassing, and no notable impact was observed from the degassing configuration in the other properties, this analysis exclusively considered the PSUs where vacuum degassing was utilized. As shown in Figure 8a, consistent trends in the F_d values can be observed, reflecting the degassing performance during the extrusion process under the various processing conditions. Accordingly, processing the material with PSU2 yields the most effective degassing performance, while PSU5 results in the poorest performance with F_d values of 41% and 15%, respectively. This suggests that an optimal degassing performance can be achieved by utilizing a fine filtration in combination with higher screw speeds and vacuum degassing.

A pronounced effect of the filtration system is evident, as switching from the F100 filtration to F140 results in a reduction in F_d by approximately 60% and 46% at 150 and 250 rpm, respectively. Additionally, with the finer filtration system F100, F_d increases by roughly 10% with increasing the screw speed from 150 to 250 rpm. This increase, proportionally, grows to around 46% with the F140 filtration system. This behavior can be attributed to varying throughput per screw revolution, influenced by the constant mass flow rate over time. Moreover, as previously illustrated (Figure 5a), increasing the screw speed causes the melt temperature to elevate, thereby reducing

the melt viscosity. Consequently, this accelerates the diffusive mass transport. Moreover, the higher screw speed enhances surface renewal, indicating that the free surfaces of the melt pool in the partially-filled screw channel renew more rapidly. These combined effects contribute to an enhanced degassing performance.^{4,69}

On the other hand, the results of the ATD-GC-MS measurements can be divided into qualitative and semi-quantitative analyzes. The qualitative analysis aims to identify the prominent compounds present in the recyclates based on the mass spectroscopy spectra, while the semi-quantitative analysis aims to compare the total VOC levels in the recyclates after being subjected to the various PSUs. Regardless of the processing conditions, the most prevalent compounds identified in the resulting recyclates are tabulated in Table 6. Recent literature studies,^{70,71} focusing on identifying prominent VOCs in plastic waste, suggest that these VOCs are commonly encountered in plastic waste and recyclates. Typically, they originate from the use phase of the product, often due to consumer's misuse of plastics, potentially resulting in material contamination during the recycling process. Additionally, some of these substances may also be introduced during recycling process due to the degradation of the polymer or certain additives.⁷²

Furthermore, the results of the semi-quantitative VOC analysis in relation to the various processing parameters are depicted in Figure 8b. Overall, a distinct correlation is evident between the VOC levels and the employed filtration system. Clearly, the finer filtration system consistently resulted in lower residual VOC contents in the recyclates. Switching from the F100 filtration to the F140 filtration

TABLE 6 List of the prominent compounds detected in the mass spectroscopy spectra of the recyclates.

Retention time [min]	Dominant peak/compounds
4.8	Heptane
5.8	Methyl isobutyl ketone
13.4	Neopentyl glycol
16.8	Decane
18.2	Limonene
29.7	Triacetin
33.9	2,6-Bis-(1,1-dimethylethyl)-phenol
37.1	1-Hydroxycyclohexyl-penyl-methanone
39.8	Methylester mexadecaic acid
40.1	Hexadecanoic acid
41.8	Methylstearate
42.1	Tributyl ester-1-propene-1,2,3-tricarboxylic acid
42.4	Butylcitrate
43.0	Tributyl acetylcitrate

led to a proportional increase in VOC levels in the corresponding recyclates, ranging from as low as a 45% increase (PSU4 to PSU8) to as high as a 145% increase (PSU3 to PSU7). This can be attributed to the higher rejection rate in the finer filtration system, which also aligns with the earlier findings where the F100 filtration enhanced degassing performance, resulting in lower residual VOC levels. When considering the impact of screw speed, it appears that with the F100 filtration, the higher screw speed resulted in increased VOC levels when combined with atmospheric degassing. However, with F140 filtration, a similar trend was observed under vacuum degassing, while the opposite pattern emerged under atmospheric degassing. As a result, it can be assumed that the impact of screw speed and degassing setup on VOC levels is somewhat arbitrary in nature. Though, it must be noted that other factors, such as the sensitivity of the analytical method, sample preparation, and variations in initial VOC levels in the input materials, which can affect VOC levels in the recyclates, may have contributed to the variability in VOC content, introducing outliers into the datasets. Nevertheless, the overall findings of this analysis suggest that the filtration system has a more pronounced effect on VOC levels compared to other processing parameters.

4 | SUMMARY AND CONCLUSIONS

As a starting point for this study, the assessment of the input PP dominated material stream, and therefore

feedstock variability, focused on AC and MFR. Samples of the input material exhibited consistent MFR values across the 10 different BBs investigated, averaging 3.8 g/10 min. Notably, the AC levels of the input materials were remarkably high, averaging around 38%, signifying the substantial presence of inorganic fillers in the materials. To investigate the influence of feedstock variability and extrusion process on the property profile of the recyclate, a two-part experimental approach was employed. In Part A, a continuous process ran for 5 h under controlled conditions with fixed extrusion parameters to assess the input material variability by monitoring the behavior of recyclate properties over time. On the other hand, Part B systematically evaluated the effects of specific processing settings, including screw speed; filtration setup; and degassing setup, on recyclate properties.

The processing of the material in Part A generally resulted in low MAD values for all properties tested, ranging from 2.8% to 6.6%, indicating a limited variability in the process. Moreover, the consistency of the data was confirmed by SPCC, where all data points fell within the control limits and followed a normal distribution around the centerline.

Under varying processing conditions in Part B, the melt temperature was primarily influenced by the screw speed, with no discernible influence from other processing configurations. This increase in melt temperature resulted in elevated MFR values. This phenomenon can be attributed to the thermomechanical degradation of the PP fraction in the material composition, leading to reduced weight average molar masses through chain scission, consequently resulting in higher MFR.^{41,43,52,63} Conversely, AC remained unaffected by processing conditions. The oxidation induction temperature demonstrated consistency across the various PSUs investigated. Mechanical properties, specifically the tensile modulus, exhibited enhancement with higher screw speeds and the use of the finer filtration setup. This increase can be associated with the higher crystallinity due to chain scission and to higher material homogeneity.^{41,43,52,63} Moreover, a positive correlation between inorganic filler content and tensile modulus was observed. The stress at yield remained relatively consistent across all processing conditions, while the strain at break decreased with increasing the screw speed. Overall, all recyclates produced exhibited relatively low Charpy NIS with no substantial influence from the processing conditions. Lastly, the most effective degassing performance was achieved through the combination of higher screw speed and finer filtration setup, which was corroborated by the lowest residual volatile organic compound levels in the resulting recyclates.

AUTHOR CONTRIBUTIONS

Mohamad Hassan Akhras: Conceptualization (equal); data curation (equal); formal analysis (equal); investigation (equal); methodology (equal); visualization (equal); writing – original draft (equal). **Christian Marschik:** Conceptualization (equal); data curation (equal); formal analysis (equal); funding acquisition (equal); investigation (equal); methodology (equal); project administration (equal); resources (equal); software (equal); writing – review and editing (equal). **Chi Nghia Chung:** Investigation (equal). **Ines Traxler:** Investigation (equal). **Konstanze Kruta:** Investigation (equal). **Karin Kloiber:** Data curation (equal); software (equal). **Joerg Fischer:** Funding acquisition (equal); methodology (equal); project administration (equal); resources (equal); supervision (lead); writing – review and editing (equal).

ACKNOWLEDGMENTS

This work was supported by the facilities at Johannes Kepler University Linz (Linz, Austria) and this article is funded by the Johannes Kepler Open Access Publishing Fund.

FUNDING INFORMATION

The authors acknowledge financial support through the COMET Centre CHASE, funded within the COMET—Competence Centers for Excellent Technologies programme by the BMK, the BMDW, and the Federal Provinces of Upper Austria and Vienna (funding number 868615). The COMET programme is managed by the Austrian Research Promotion Agency (FFG).

DATA AVAILABILITY STATEMENT

The data presented in this study are available on request from the corresponding authors.

ORCID

Mohamad Hassan Akhras  <https://orcid.org/0000-0002-1246-8941>

Christian Marschik  <https://orcid.org/0000-0003-2033-9047>

Ines Traxler  <https://orcid.org/0000-0001-8205-4798>

Joerg Fischer  <https://orcid.org/0000-0002-1047-3085>

REFERENCES

- [1] K. Ragaert, L. Delva, K. van Geem, *Waste Manag.* **2017**, *69*, 24.
- [2] The European Parliament and The Council of the European Union. Directive 2008/98/EC of the European Parliament and of the Council of 19 **2008** on waste and repealing certain Directives. <https://eur-lex.europa.eu/legal-content/EN/TXT/?uri=celex%3A32008L0098>.
- [3] The European Parliament and The Council of the European Union. *DIRECTIVE (EU) 2018/851 OF THE EUROPEAN PARLIAMENT AND OF THE COUNCIL: amending Directive 2008/98/EC on waste.* <https://eur-lex.europa.eu/legal-content/EN/TXT/?uri=celex%3A32018L0851>.
- [4] C. N. Chung, C. Marschik, J. Klimosek, J. Kosek, M. H. Akhras, G. Steinbichler, *Recycling* **2023**, *8*, 72.
- [5] Deutschen Instituts für Normung, Classification of recycled plastics by Data Quality Levels for use and (digital) trading, (DIN SPEC 91446). **2021** <https://www.din.de/en/wdc-beuth:din21:340423834?destinationLanguage=&sourceLanguage=>
- [6] S. M. Al-Salem, P. Lettieri, J. Baeyens, *Waste Manag.* **2009**, *29*, 2625.
- [7] I. A. Ignatyev, W. Thielemans, B. Vander Beke, *ChemSusChem* **2014**, *7*, 1579.
- [8] International Standardization Organization, Plastics – Guidelines for the recovery and recycling of plastics waste, (ISO 15270). **2008** <https://www.iso.org/standard/45089.html>
- [9] I. Antonopoulos, G. Faraca, D. Tonini, *Waste Manag.* **2021**, *126*, 694.
- [10] S. Yin, R. Tuladhar, F. Shi, R. A. Shanks, M. Combe, T. Collister, *Polym. Eng. Sci.* **2015**, *55*, 2899.
- [11] Z. O. G. Schyns, M. P. Shaver, *Macromol. Rapid Commun.* **2021**, *42*, e2000415.
- [12] J. Maris, S. Bourdon, J.-M. Brossard, L. Cauret, L. Fontaine, V. Montebault, *Polym. Degrad. Stab.* **2018**, *147*, 245.
- [13] S. M. Alshahrani, J. T. Morott, A. S. Alshetaili, R. V. Tiwari, S. Majumdar, M. A. Repka, *Eur. J. Pharm. Sci.* **2015**, *80*, 43.
- [14] C. Marschik, B. Löw-Baselli, J. Miethlinger, Modeling devolatilization in single- and multi-screw extruders. Proceedings Of Pps-32: The 32nd International Conference of the Polymer Processing Society—Conference Papers, 29 July 2016. **2017**.
- [15] S. Pachner, W. Roland, M. Aigner, C. Marschik, U. Stritzinger, J. Miethlinger, *Int. Polym. Process.* **2021**, *36*, 435.
- [16] F. P. La Mantia, *Prog. Rubber. Plast. Re.* **2004**, *20*, 11.
- [17] A. Schweighuber, A. Felgel-Farnholz, T. Bögl, J. Fischer, W. Buchberger, *Poly. Degrad. Stab.* **2021**, *192*, 109689.
- [18] EREMA Engineering Recycling. INTAREMA TVEplus: Recycling system with high-performance degassing. https://www.ereama.com/en/intarema_tveplus/.
- [19] M. H. Akhras, J. Fischer, *Polymers.* **2022**, *14*(17), 3450. <https://doi.org/10.3390/polym14173450>
- [20] International Standardization Organization, *Plastics - Polypropylene (PP) moulding and extrusion materials - Part 2: Preparation of test specimens and determination of properties* (ISO 19069-2). **2016** <https://www.iso.org/standard/66828.html>
- [21] International Standardization Organization, *Plastics - Injection moulding of test specimens of thermoplastic materials - Part 1: General principles, and moulding of multipurpose and bar test specimens* (ISO 294-1). <https://www.iso.org/standard/67036.html>
- [22] International Standardization Organization, *Plastics – Multi-purpose test specimens* (ISO 3167). **2014** <https://www.iso.org/standard/65105.html>
- [23] International Standardization Organization, *Plastics – Determination of Charpy impact properties – Part 1: Non-instrumented impact test* (ISO 179-1). **2010** <https://www.iso.org/standard/44852.html>
- [24] International Standardization Organization, *Plastics – Standard atmospheres for conditioning and testing* (ISO 291). **2008** <https://www.iso.org/standard/50572.html>

- [25] International Standardization Organization, *Plastics – Determination of the melt mass-flow rate (MFR) and melt volume-flow rate (MVR) of thermoplastics – Part 1: Standard method* (ISO 1133-1). **2022** <https://www.iso.org/standard/83905.html>
- [26] S. Möllnitz, M. Feuchter, I. Duretek, G. Schmidt, R. Pomberger, R. Sarc, *Polymers*. **2021**, *13*(3), 457. <https://doi.org/10.3390/polym13030457>
- [27] M. Gall, G. Steinbichler, R. W. Lang, *Mater. Des.* **2021**, *202*, 109576.
- [28] International Standardization Organization, *Plastics – Determination of ash – Part 1: General methods* (ISO 3451-1). **2019** <https://www.iso.org/standard/71205.html>
- [29] International Standardization Organization, *Plastics – Differential scanning calorimetry (DSC) – Part 1: General principles* (ISO 11357-1). **2016** <https://www.iso.org/standard/70024.html>
- [30] International Standardization Organization, *Plastics – Differential scanning calorimetry (DSC) – Part 6: Determination of oxidation induction time (isothermal OIT) and oxidation induction temperature (dynamic OIT)* (ISO 11357-6). **2018** <https://www.iso.org/standard/72461.html>
- [31] International Standardization Organization. *Plastics – Determination of tensile properties – Part 1: General principles* (ISO 527-1), **2019**. <https://www.iso.org/standard/75824.html>.
- [32] International Standardization Organization. *Plastics – Determination of tensile properties – Part 2: Test conditions for moulding and extrusion plastics* (ISO 527-2), **2012**. <https://www.iso.org/standard/56046.html>.
- [33] A. Király, F. Ronkay, *Polym. Polym. Compos.* **2013**, *21*, 93.
- [34] T. Thenepalli, A. Y. Jun, C. Han, C. Ramakrishna, J. W. Ahn, *Korean J. Chem. Eng.* **2015**, *32*, 1009.
- [35] K. Palanikumar, R. AshokGandhi, B. K. Raghunath, V. Jayaseelan, *Materials Today: Proceedings* **2019**, *16*, 1363.
- [36] A. V. Shenoy, *Rheology of Filled Polymer Systems*, Springer Netherlands, Dordrecht **1999** ISBN 978-90-481-4029-9.
- [37] S. Djellali, L. Djahnit, H. Ferkous, *Mater. Biomater. Sci.* **2020**, *3*, 40–45.
- [38] W. A. Shewhart, W. E. Deming, *Statistical method from the viewpoint of quality control*, Dover Publications, Inc, New York **1986** ISBN 9780486652320.
- [39] Y. Y. Cheung, B. Jung, J. H. Sohn, G. Ogrinc, *Radiographics* **2012**, *32*, 2113.
- [40] M. H. Akhras, J. Langwieser, J. Fischer, Investigation of the degradative impact of multiple reprocessing loops on the rheological behavior of different polypropylenese. proceedings of the 37th international concerence of polymer processing society (PPS-37), AIP Publishing, Fukuoka, Japan. **2023**.
- [41] J. Aurrekoetxea, M. A. Sarrionandia, I. Urrutibeascoa, M. L. Maspoch, *J. Mater. Sci.* **2001**, *36*, 2607.
- [42] H. Cornier-Ríos, P. A. Sundaram, J. T. Celorie, *J. Polym. Environ.* **2007**, *15*, 51.
- [43] A. Santos, J. Agnelli, D. Trevisan, S. Manrich, *Polym. Degrad. Stab.* **2002**, *77*, 441.
- [44] H. Hinsken, S. Moss, J.-R. Pauquet, H. Zweifel, *Polym. Degrad. Stab.* **1991**, *34*, 279.
- [45] S. Saikrishnan, D. Jubinville, C. Tzoganakis, T. H. Mekonnen, *Polym. Degrad. Stab.* **2020**, *182*, 109390.
- [46] H. B. Parmar, R. K. Gupta, S. N. Bhattacharya, *Polym. Eng. Sci.* **2009**, *49*, 1806.
- [47] H. Jin, J. Gonzalez-Gutierrez, P. Oblak, B. Zupančič, I. Emri, *Polym. Degrad. Stab.* **2012**, *97*, 2262.
- [48] L. A. Pinheiro, M. A. Chinelatto, S. V. Canevarolo, *Polym. Degrad. Stab.* **2004**, *86*, 445.
- [49] M. Loutcheva, M. Proietto, N. Jilov, F. P. La Mantia, *Polym. Degrad. Stab.* **1997**, *57*, 77.
- [50] T. Kealy, *J. Appl. Polym. Sci.* **2009**, *112*, 639.
- [51] S. Apone, R. Bongiovanni, M. Braglia, D. Scalia, A. Priola, *Polym. Test.* **2003**, *22*, 275.
- [52] H. M. Da Costa, V. D. Ramos, M. G. d. Oliveira, *Polym. Test.* **2007**, *26*, 676.
- [53] L. Shen, G. D. Gorbea, E. Danielson, S. Cui, C. J. Ellison, F. S. Bates, *Proc. Natl. Acad. Sci. USA* **2023**, *120*, e2301352120.
- [54] J. Vera-Sorroche, A. Kelly, E. Brown, P. Coates, N. Karnachi, E. Harkin-Jones, K. Li, J. Deng, *Appl. Therm. Eng.* **2013**, *53*, 405.
- [55] H. T. Kim, E. A. Collins, *Polym. Eng. Sci.* **1971**, *11*, 83.
- [56] O. S. Carneiro, J. A. Covas, B. Vergnes, *J. Appl. Polym. Sci.* **2000**, *78*, 1419.
- [57] M. Peltzer, A. Jiménez, *J. Therm. Anal. Calorim.* **2009**, *96*, 243.
- [58] A. T. P. Zahavich, B. Latto, E. Takacs, J. Vlachopoulos, *Adv. Polym. Technol.* **1997**, *16*, 11.
- [59] H. J. Oswald, E. Turi, *Polym. Eng. Sci.* **1965**, *5*, 152.
- [60] F. P. La Mantia, M. Morreale, Z. A. M. Ishak, *J. Appl. Polym. Sci.* **2005**, *96*, 1906.
- [61] K. Yang, Q. Yang, G. Li, Y. Sun, D. Feng, *Polym. Compos.* **2006**, *27*, 443.
- [62] M. J. Zaini, M. Y. A. Fuad, Z. Ismail, M. S. Mansor, J. Mustafah, *Polym. Int.* **1996**, *40*, 51.
- [63] S. V. Canevarolo, *Polym. Degrad. Stab.* **2000**, *70*, 71.
- [64] M. Gall, P. J. Freudenthaler, J. Fischer, R. W. Lang, *Polymers (Basel)* **2021**, *13*(10), 1574. <https://doi.org/10.3390/polym13101574>
- [65] P. Supaphol, W. Harnsiri, J. Junkasem, *J. Appl. Polym. Sci.* **2004**, *92*, 201.
- [66] S. M. Zebarjad, M. Tahani, S. A. Sajjadi, *J. Mater. Process. Technol.* **2004**, *155–156*, 1459.
- [67] Y. W. Leong, M. B. Abu Bakar, Z. A. M. Ishak, A. Ariffin, B. Pukanszky, *J. Appl. Polym. Sci.* **2004**, *91*, 3315.
- [68] S.-F. Zeng, Y. Zeng, P. Guo, C.-Y. Hu, Z.-W. Wang, *Polym. Degrad. Stab.* **2023**, *208*, 110263.
- [69] C. Marschik, B. Löw-Baselli, J. Miethlinger, *Int. Polym. Process.* **2017**, *32*, 387.
- [70] A. Cabanes, F. J. Valdés, A. Fullana, *Sustain. Mater. Technol.* **2020**, *25*, e00179.
- [71] R. Demets, M. Roosen, L. Vandermeersch, K. Ragaert, C. Walgraeve, S. de Meester, *Resour. Conserv. Recycl.* **2020**, *161*, 104907.
- [72] S. Palkopoulou, C. Joly, A. Feigenbaum, C. D. Pappaspyrides, P. Dole, *Trends Food Sci. Technol.* **2016**, *49*, 110.

How to cite this article: M. H. Akhras, C. Marschik, C. N. Chung, I. Traxler, K. Kruta, K. Kloiber, J. Fischer, *J. Appl. Polym. Sci.* **2024**, e55731. <https://doi.org/10.1002/app.55731>